A Comparative Study between the FFT and DWT Method Applied to a Bearing Fault in Induction Motors – Results Dedicated to the Industry –

N. BESSOUS[1,2], S. E. ZOUZOU[1], W. BENTRAH [3], S. SBAA[3]

[1] Department of Electrical Engineering, Laboratory LGEB, Med Khider University 07000 Biskra.

[2] Department of Electrical Engineering, University of El-Oued, 39000 Algeria.

[3] Department of Electronics, LI3CUB Laboratory, Med Khider University 07000 Biskra.

Biskra, Algeria

nbessous@yahoo.fr zouzou_s@hotmail.com wafaelect@gmail.com s_sbaa@yahoo.fr

Abstract: - The diagnosis of rotating machines by signals analysis has evolved considerably in recent years thanks to advanced signal processing techniques.

The bearing faults have an important percentage by comparison with the stator or rotor faults in induction machines. The method used to detect this defect is based on accurate and clear information at any time.

In addition to that, many works have dealt with the diagnosis by several techniques.

Our work will deal with two approach signals that are used for bearing fault diagnosis:

1- The first is based on the fast Fourier transform (FFT), by using the spectral analysis of the stator current. The accuracy of this method depends on the following conditions: invariable load and constant speed.

2- The second method is based on the discrete wavelet transform (DWT), which is regarded as a tool for analyzing the variable signals.

These two approaches are applied to the experimental results, through an analysis of the stator current, only to find a clear defect and accurate information.

Key-Words: - Bearing defect, Discrete wavelet transform (DWT), Fault diagnosis, Induction motors, Inner raceway, Outer raceway, Spectral analyses (FFT).

1 Introduction

The precocious detection of anomaly in the induction motor helps us to avoid future serious damage. The air-gap between the stator and rotor in the good machine is equal. But under other different circumstances; eccentricity (static or dynamic), bearing defect, etc, the value of air-gap becomes unequal. In the last case of bearing fault, the axis of the rotor rotation does not coincide with the center of the stator.

The bearing (rolling) is constituted of four parts, these different elements define the variety of the faults that can attack the bearing itself. The elements are: outer race, inner race, cage and balls. In this paper, we are going to detect the defect of the outer and inner raceway by using two methods.

The first one is the motor current signature analysis (MCSA) by fast Fourier transform (FFT). This method has some advantages like the simplicity of the current measuring. This later will be discussed by using the FFT.

This technique has been used by several researchers in order to extract adequate information. The eccentricity of the machine is a defect caused by the changeable air-gap that exists between the stator and rotor [1-4]. Eccentricity fault has several origins as improper placement during assembly, a defect of the shaft, and so forth.

The authors [5-7] study the defect of broken bars by MCSA analysis, which is used to detect the bearing defect [9-10].

The appearance or the disappearance of new harmonics, and the increase or the decrease of the amplitude are considered as information helping for detecting the defect [11]. The signal given by the probes of the current must be analyzed correctly in healthy and faulty conditions [3], [6], [9].

Therefore, this technique is based on the monitoring of stator current specters.

The second technique called discrete wavelet transform; it was applied by many researchers on asynchronous machines. The reference [12]

analyzed the stator current via wavelet transform to detect bearing defects; applying wavelet transform.

The diagnosis of rotor defects was carried out by [13, 14] for a healthy and defective machine.

A proposal based on the discrete wavelet transform (DWT) in order to detect failures in the rotor bars in induction machines, by analyzing the stator current [15, 16].

Finally, the analysis is performed by the MCSA and DWT for an induction machine, and under a defect of outer and inner race; our obtained results will be compared and discussed.

2 Application of the FFT Technique

The experimental studies were applied on a machine which is characterized of 3 phases, 50 Hz, 380 V, 3kW, 28 rotor bars and 2 pole pairs. The induction motor is triangle-connected with a rotor carried by two bearings, one of which is defective in the outer and in the inner raceway.

The experimental setup is shown in Fig. 1. The line current is measured and recorded by D-space carte 1104. After acquisition, the data were processed using MATLAB software package to calculate and analyze the signal.

Fig. 1 Experiment setup for bearing fault

2.1 Analysis of the stator current spectrum

When including a subsection you must use, for its heading, small letters, 12pt, left justified, bold, Times New Roman as here.

The method is employed to test the efficiency of the stator current analysis. The bearing fault detection lies on the experimental comparison between the spectra of the current in healthy, faulty, full load or no-load conditions.

The frequencies appear in the spectra of stator current are verified by the following formula:

$$f_{bearing\ defect} = |f_{su} \pm k.f_c| \quad (1)$$

where $k = 1, 2, 3, \ldots$, f_c is one of the characteristic frequencies, f_{su} is the supply frequency, and $f_{bearing\ defect}$ is the bearing fault frequencies reflected in the stator current.

The bearing geometry (Fig. 2) and the mechanical rotor frequency f_r led us to write the different formulas of the characteristic frequencies f_c as [17, 18, 19, 20]:

Outer raceway:

$$f_c = f_o = \frac{N_b}{2} f_r \left(1 - \frac{D_b}{D_c} \cos\beta\right) \quad (2)$$

Inner raceway:

$$f_c = f_i = \frac{N_b}{2} f_r \left(1 + \frac{D_b}{D_c} \cos\beta\right) \quad (3)$$

Ball:

$$f_c = f_b = \frac{D_c}{D_b} f_r \left(1 - \frac{D_b^2}{D_c^2} \cos^2\beta\right) \quad (4)$$

It has been statistically shown in [8] that the vibration frequencies can be approximated for most bearings with balls between 6 and 12 by:

$$f_c = f_o = 0.4 N_b . f_r \quad (5)$$

$$f_c = f_i = 0.6 N_b . f_r \quad (6)$$

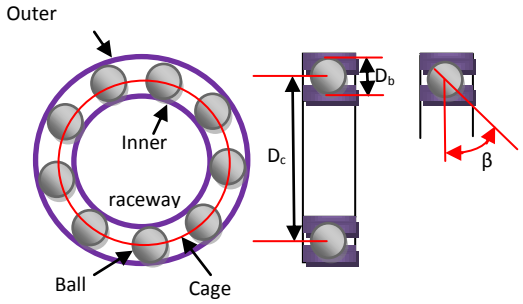

Fig. 2 Ball bearing parameters

2.2 Outer race defect

Figure 3 below illustrates the characteristic frequencies of the outer race compared to the healthy state of the machine and under a load equal to 0nm (at no-load).

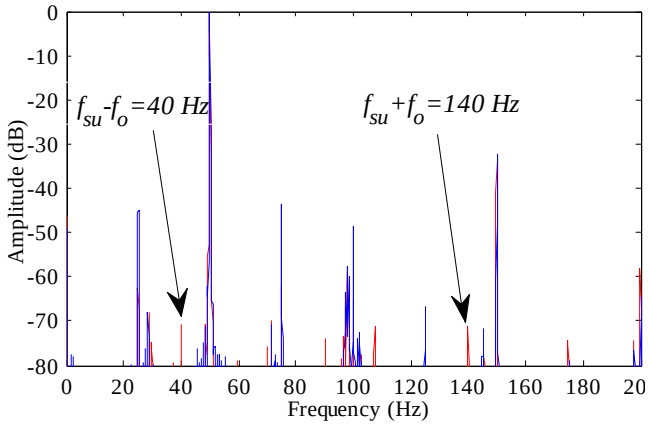

Fig. 3 Stator current spectrum of healthy (blue) and faulty (red) motor at no load (s=0)

These results are confounded with the formula of characteristic frequencies of the defect; without forgetting to take in consideration the phenomena to the tests that influence for example to the slip also.

$$f_{Or1} = |f_{su} - f_c| = |f_{su} - 0.4N_b f_r| = 40\,Hz$$
$$f_{Or2} = |f_{su} + f_c| = |f_{su} + 0.4N_b f_r| = 140\,Hz$$

The characteristic frequencies are so clear in comparison with the healthy state. The machine is operating at full load (Fig. 4).

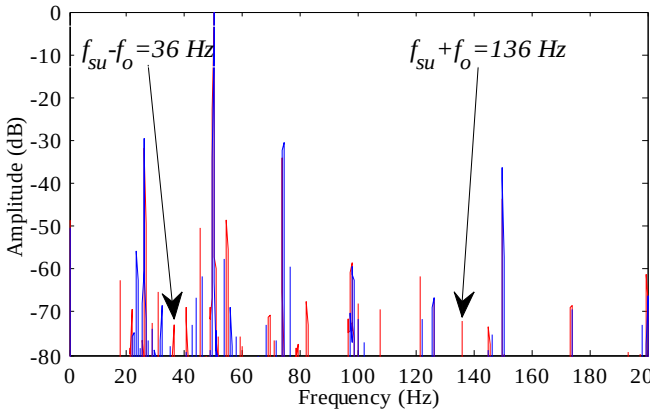

Fig. 4 Stator current spectrum of healthy (blue) and faulty (red) motor at full load (s=0.044)

according to the FFT of the current writes to some:

$$f_{Or1} = 36\,Hz,\ \ Amp = -73.16\,dB$$
$$f_{Or2} = 136\,Hz,\ \ Amp = -72.29\,dB$$

and by verification of the formula:

$$f_{Or1} = |f_{su} - f_c| = |f_{su} - 0.4N_b f_r| = 36.04\,Hz$$
$$f_{Or2} = |f_{su} + f_c| = |f_{su} + 0.4N_b f_r| = 136.04\,Hz$$

2.3 Inner race defect

It can be noted in Fig. 5 and Fig. 6, the stator current spectrum in the presence of a defect. We see the appearance of harmonic peaks at frequencies characteristic of the inner race defects for different conditions (no-load and full load). However, note that all possible combinations of characteristic frequencies exist.

The frequencies characteristics in this case are:

$$f_{Ir1} = 84.6\,Hz,\ \ Amp = -63.26\,dB$$
$$f_{Ir2} = 184.6\,Hz,\ \ Amp = -66.42\,dB$$

These results are confounded also with the formula of characteristic frequencies of the defect.

$$f_{Ir1} = |f_{su} - f_c| = |f_{su} - 0.4N_b f_r| = 84.46\,Hz$$
$$f_{Ir2} = |f_{su} + f_c| = |f_{su} + 0.4N_b f_r| = 184.46\,Hz$$

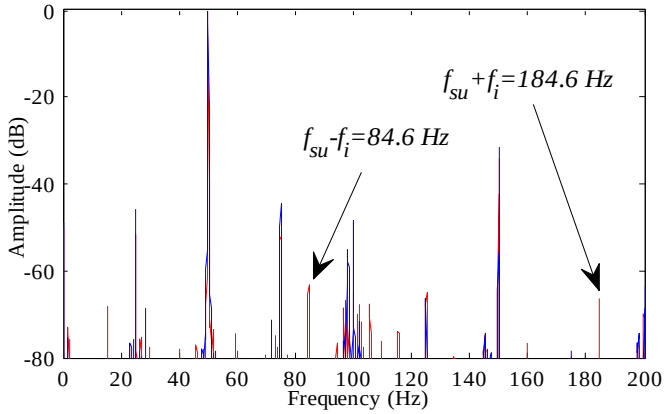

Fig. 5 Stator current spectrum of healthy (blue) and faulty (red) motor at no load (s=0.004)

according to the FFT of the current writes to some:

$$f_{Ir1} = 78.6\,Hz,\ \ Amp = -66.2\,dB$$
$$f_{Ir2} = 178.6\,Hz,\ \ Amp = -65.54\,dB$$

and by verification of the formula:

$$f_{Ir1} = |f_{su} - f_c| = |f_{su} - 0.4N_b f_r| = 79.06\,Hz$$
$$f_{Ir2} = |f_{su} + f_c| = |f_{su} + 0.4N_b f_r| = 179.06\,Hz$$

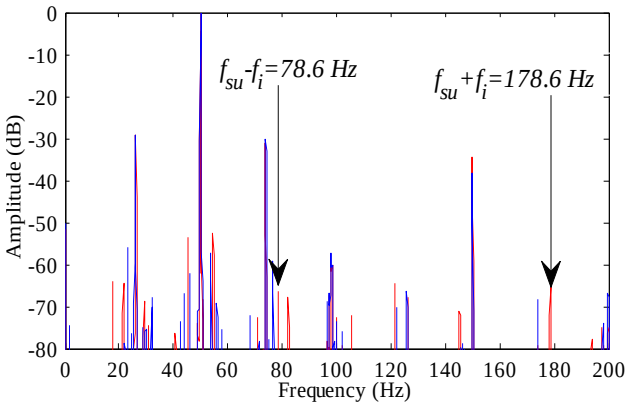

Fig. 6 Stator current spectrum of healthy (blue) and faulty (red) motor at full load (s=0.044)

Note also that the detection of bearing failures could be done by analyzing the spectral content of the stator current.

3 Application of the DWT Technique

The discrete wavelet transform (DWT) can make a time-frequency representation of a non-stationary signal with higher resolution time. The effectiveness of this technique is remarkable. The generalization of Fourier transforms short time (STFT) has a constant length of the window.

DWT is the decomposition of a signal by basing a successive transition from a high-pass filter, and another low pass that leads us to find the approximate and details.

LP is the abbreviation of: low-pass filter, while HP refers to the high-pass filter. The first level of decomposition coefficients is a1 one and the other d1. a1 is the approximate shape of the original signal and d1 is the detailed shape of the original signal. Moreover decomposition produces two coefficients a1, a2 are also and d2, as shown here a1, a2 approach more of the original signal Fig. 7.

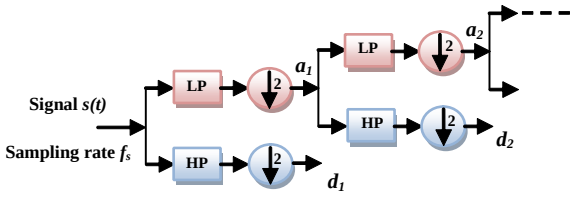

Fig. 7 Discrete wavelet decomposition process

These decompositions are limited by the number; limited number of levels is defined by [15]:

$$N_{LL} = \text{int}\left[\frac{\log\left(\frac{f_s}{f_{su}}\right)}{\log(2)}\right] \quad (7)$$

f_s, f_{su} the sampling frequency and fundamental frequency respectively.

Indicating that [15] proposed a different number of levels for adequate analysis, it adds 2 to N_{LL}.

Therefore for a frequency of sampling of 10 KHz, the number of decomposition, advisable is of:

$$N_{Ls} = \text{int}\left[\frac{\log\left(\frac{10\times10^3}{50}\right)}{\log(2)}\right] + 2 = 9 \; levels$$

Apiece of the wavelet scales corresponds to a frequency band f given by [21]

$$f_{hb} = 2^{(n-m)}\left(\frac{f_s}{2^n}\right) \quad (8)$$

where f_{hb} is the higher frequency limit of the frequency band represented by decomposition level m, f_s is the sampling frequency, and 2^n is the number of data points in the signal.

The tree of decomposition of a signal with the frequency bands can be represented as:

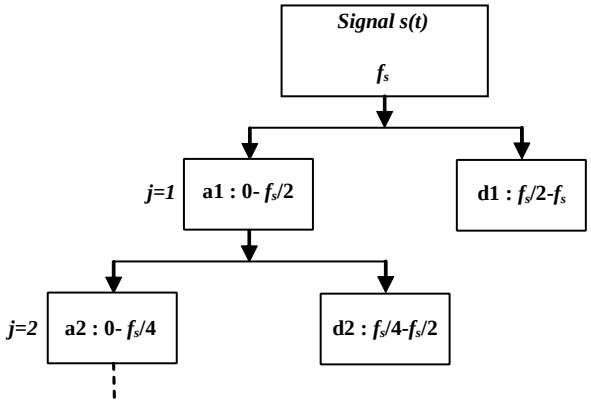

Fig. 8 Flowchart frequency bands

The table 1 indicates the different frequency bands obtained from the decomposition of discrete wavelet.

Table.1 Frequency bands at different decomposition levels

Frequency bands of levels (Hz)	
d1	5000-10000
d2	2500-5000
d3	1250-2500
d4	625-2500
d5	312.5-625
d6	156.25-312.5
d7	78.125-156.25
d8	39.0625-78.125
d9	19.53-39.0625

3.1 Outer race defect

The explanation shows that the use of both wavelet Debauchies and Dmey, gives the same result. Manu researchers [15] applied the wavelet Debauchies to analyze the faults.

The choice of the mother wavelet plays a very important role in obtaining adequate results. Our study is a part of several types (Daubechies, Dmey, Simlet, Coiflet, Haar, ...). We find that the mother wavelet Daubechies and Dmey give more precise details signals and fewer harmonics.

We also tested the steps of the wavelet mother herself; that is to say, db20, db21, db40, …, and db45, according to these tests. According to the previous analysis, we should indicate that obtaining adequate results requires the order of Daubechies to be more than 40.

The order of Daubechies plays a very important role for many reasons, and one of those advantages is the possibility to detect the information of the fault view (for the eyes) to the high-level details. The stator current signals have a smooth form (theoretically) in the healthy machine, so that all changes of current can be detected easily.

In our case, we have chosen Daubechies-43 as the mother wavelet for the DWT analysis.

When we exceed the maximum wavelet decomposition level, the signal shape will be far from the original one. In order to keep the original shape of the signal, we should stop at the sixth level to analyze the signals; we must find the difference between the two cases (healthy and faulty machine). In general, d8 and d9 are smooth, so that all changes happened can be detected.

We will take the details and one approximation (a9), plus the original signal current. These results are for a healthy machine (Fig. 9) and bearing defect defective (outer race) (Fig. 10), the machine is 0% load.

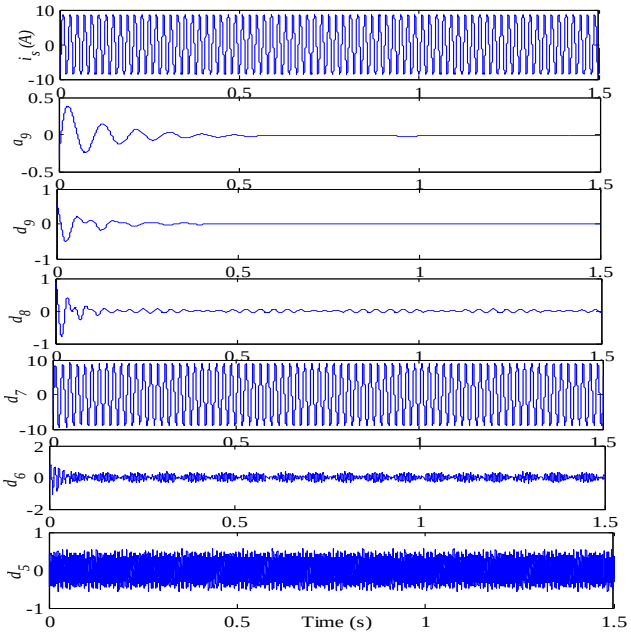

Fig. 9 Level wavelet signals results from the DWT signal analysis of experimental stator current in healthy machine (0% load)

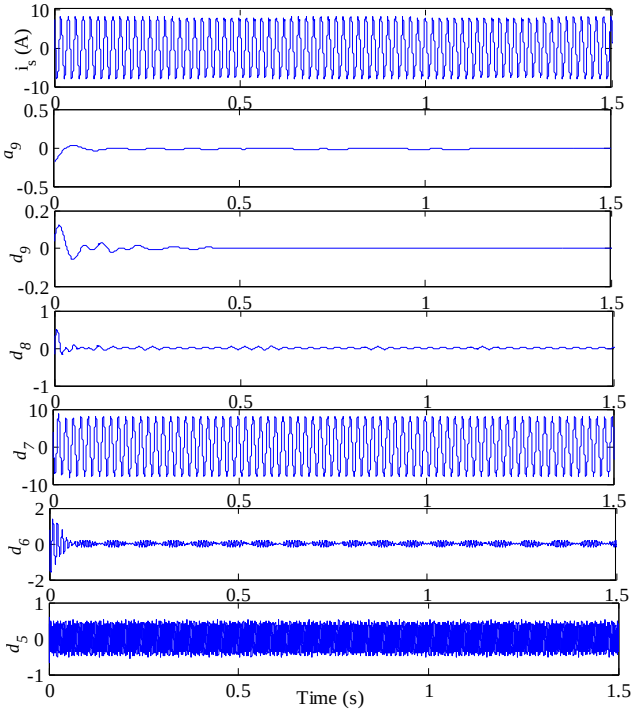

Fig. 10 Level wavelet signals results from the DWT signal analysis of experimental stator current in faulty case (outer race, 0% load)

We take like an indicator of defect the energy, this last concentrated in every level of the detail of decomposition of the wavelet. Hereby is the calculation of the energy of details at level *j* is given by:

$$E_j = \sum_{n=1}^{N} \left| d_j(n) \right|^2 \quad (9)$$

where *j* is the level of detail, d*j* is the detail signal at level *j* and *N* is the total number of samples in the signal.

In the literature, the comparison of the energy for the two cases stops to the last level. The signal of detail d7 is closed to original shape of the signal; it shows the high value (considerable) energy to level 7. As a result, we stop at d6 in order to find the information of the defect (Fig. 11 and Fig. 12).

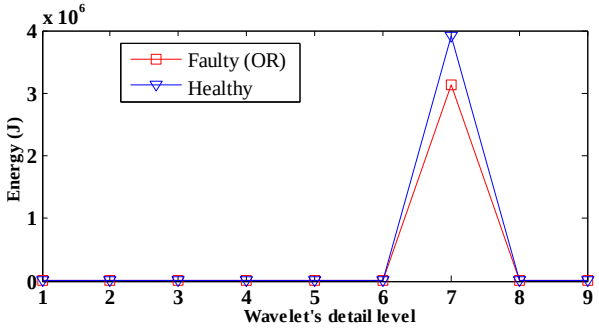

Fig. 11 Total energy corresponding to stator current in healthy and at no-load machine

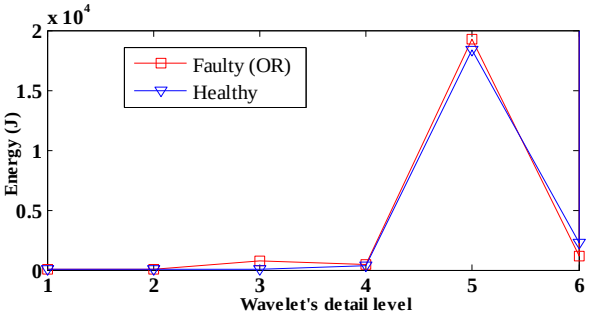

Fig. 12 Energy level from 1 to 6 corresponding to stator current in healthy and at no-load machine

We see a remarkable difference between the energy in the healthy and faulty machine. We can say that this difference is a result of the of the outer race fault. It is shown in the decrease energy, particularly at level 7.

Another fault influence of the outer ring was appeared at level 5. The influence here is reversed, i.e. it has more energy compared to healthy state (Fig. 12).

It is necessary to discuss at this point the important contribution of the d5 compared to the other, except that 7.

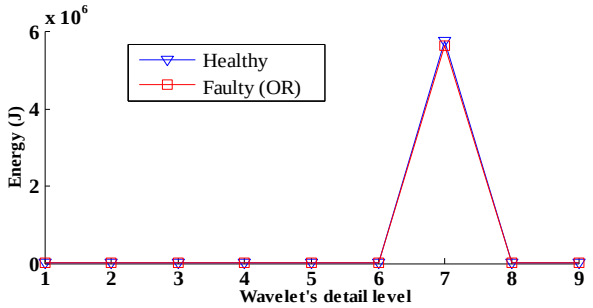

Fig. 13 Total energy corresponding to stator current in healthy and at full load machine

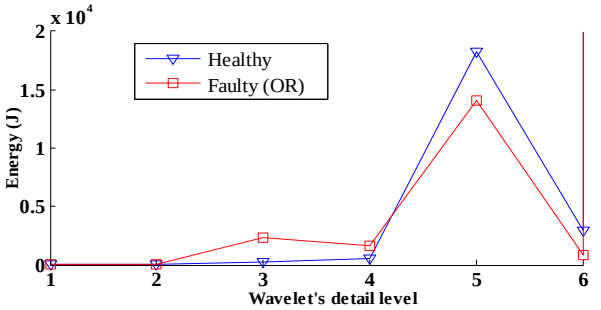

Fig. 14 Energy level from 1 to 6 corresponding to stator current in healthy and at no- load machine

When the machine is in charge, we see almost confounded energies at 7 against a remarkable variation in levels 3 and 5. It is said that the fault information by comparing energy appears at 3 and 5 (Fig. 14).

Even here, indicating the importance of the contribution of the d5 and a value less for d3 which it appears is in charge only.

3.2 Inner race defect

In the same way as bearing defect analysis at the outer race; except that we only discuss energy as a fault signal indicator.

The defect of the inner race is totally different than the first fault; that is to say, the air-gap variations caused by the two are not the same.

For the same condition, a difference in energy value is seen when comparing figures 11, 12, 13, 14 with 15, 16, 17, and 18 one by one.

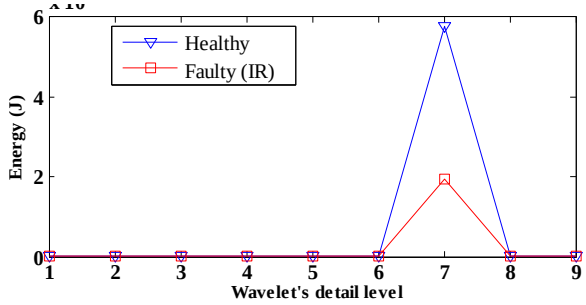

Fig. 15 Total energy corresponding to stator current in healthy and at no-load machine

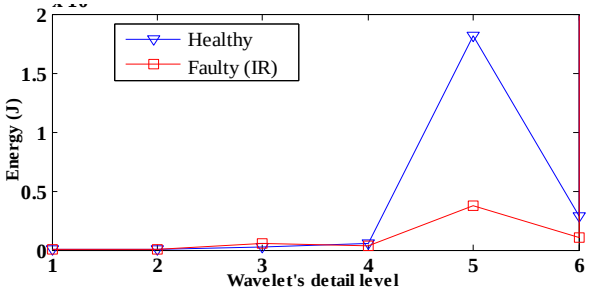

Fig. 16 Energy level from 1 to 6 corresponding to stator current in healthy and at no-load machine

The figures 17 and 18, show a significant difference in energy, so the fault information is very clear.

We note that level 5 has an important contribution to energy, therefore it may be considered as indication (information) fault detection in induction machines.

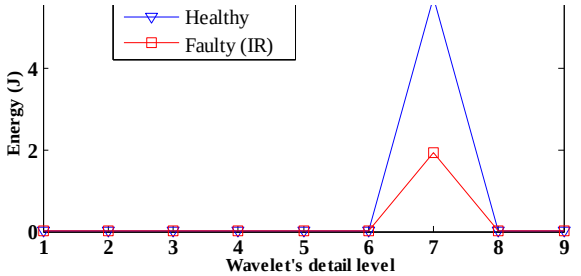

Fig. 17 Total energy corresponding to stator current in healthy and at full load machine

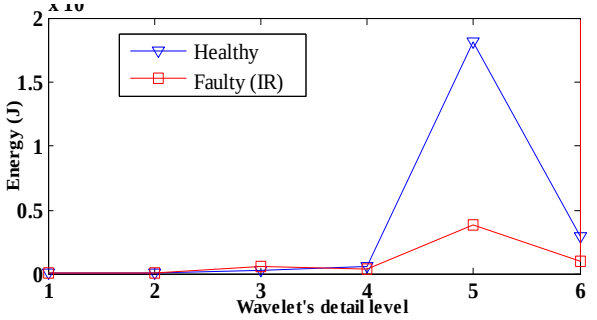

Fig. 18 Energy level from 1 to 6 corresponding to stator current in healthy and at full load machine

4 Conclusion

The bearings faults generally cause more mechanical effects in machines such as increased noise levels and vibrations. The bearing defects induce variations in the load torque of the asynchronous machine.

In this work, we have studied the feasibility of detection of bearing defects in an induction machine, based on analysis of stator currents, by using two methods.

The first is FFT and the second is DWT, both techniques treat the signature and give us rich and clear information of the fault signal.

Therefore, other problem is seen in the transitional phenomenon, through a couple of a variable load, which led to non-stationary signals. In this case, the FFT cannot analyze such signals.

To overcome this problem, the analysis of the envelope of the transient starting-current waveform using the wavelet transform can be discussed.

This study concluded that the FFT is a good method to analyze motor faults over invariable load, but in case of a variable load, an improvement is needed. Wavelets decomposition is the accurate technique for non stationary signals.

Finally, we note that electrical machine under different faults can be studied with the variable load torque.

References:

[1] J. Faiz, B. M. Ebrahimi, B. Akin. H. A. Toliyat, *Comprehensive eccentricity fault diagnosis in induction motors using finite element method*. IEEE Transactions on Magnetics, Vol. 45, No. 3, 2009, pp. 1764-1767.

[2] K. N. Gyftakis, J. C. Kappatou, *A novel and effective method of static eccentricity diagnosis in three-phase psh induction motors*. IEEE Transactions on Energy Conversions, Vol. 28, No. 2, 2013, pp. 405-412.

[3] M. Sahraoui, A. Ghoggal, S. E. Zouzou, M.E. Benbouzid, *Dynamic eccentricity in squirrel cage induction motors –simulation and analytical study of its spectral signatures on stator currents*. Simulation Modelling Practice and Theory, Vol. 16, No. 9, 2008, pp. 1503-1513.

[4] W. T. Thomson, D. Rankin and D. G. Dorrell, *On-line current monitoring to diagnose air-gap eccentricity in large three-phase induction motors-industrial case histories verify the predictions*. IEEE Transactions on Energy Conversions, Vol. 14, No. 4, 1999, pp. 1372-1378.

[5] Humberto Henao, Hubert Razik and Gérard-André Capolino, *Analytical approach of the stator current frequency harmonics computation for detection of induction machine rotor faults*. IEEE Transactions on Industry Applications, Vol. 41, No. 3, 2005, pp. 801-807.

[6] W. T. Thomas and M. Fenger, *Current signature analysis to detect induction motor faults*. IEEE Industry Applications Magazine, Vol. 7, No. 4, 2001, pp. 26–34.

[7] M. E. H. Benbouzid and G. B. Kliman, *What stator current processing based technique to use for induction motor rotor faults diagnosis?* IEEE Transactions on Energy Conversions, Vol. 18, No. 2, 2003, pp. 238–244.

[8] R. R. Schoen, T. G. Habetler, F. Kamran and R. Bartheld, *Motor bearing damage detection using stator current monitoring*. IEEE Transactions on Industry Applications, Vol. 31, No. 6, 1995, pp. 1274–1279.

[9] B. Yazici and G. B. Kliman, *An adaptive statistical time–frequency method for detection of broken bars and bearing faults in motors using stator current*. IEEE Transactions on Industry Applications, Vol. 35, No. 2, 1999, pp. 442–452.

[10] M. Blödt, P. Granjon, B. Raison and G. Rostaing, *Models for bearing damage detection in induction motors using stator current monitoring*. IEEE Transactions on Industry Applications, Vol. 55, No. 4, 2008, pp. 1813-1822.

[11] A. Bellini, F. Filippetti, G. Franceschini, C. Tassoni and G. B. Kliman, *Quantitative evaluation of induction motor broken bars by means of electrical signature analysis*. IEEE Transactions on Industry Applications, Vol. 37, No. 5, 2001, pp. 1248-1255.

[12] L. Eren, and M. J. Devaney, *Bearing damage detection via wavelet packet decomposition of the stator current*. IEEE Transactions on Instrumentation and Measurement,Vol. 53, No. 2, 2004, pp. 431 – 436.

[13] T. W. S. Chow and S. Hai, *Induction machine fault diagnostic analysis with wavelet technique*. IEEE Transactions on Industry Electronics, Vol. 51, No. 3, 2004, pp. 558–565.

[14] Kia, S. H., Henao, H. and G.A Capolino, *Diagnosis of broken-bar fault in induction machines using discrete wavelet transform without slip estimation*. IEEE Transactions on Industry Applications, Vol.45, No.4, 2009, pp. 1395-1404.

[15] Jose A. Antonino-Daviu, Martin Riera-Guasp, José Roger Folch and M. Pilar Molina Palomares, *A method for the diagnosis of rotor bar failures in induction machines*. IEEE Transactions on Industry Applications, Vol. 42, No. 4, 2006, pp. 990-996.

[16] A. Ordaz-Moreno, R.J. Romero-Troncoso, J.A. Vite-Frias, J.R. Rivera-Gillen and A. Garcia-Perez, *Automatic online diagnosis algorithm for broken-bar detection on induction motors based on discrete wavelet transform for FPGA implementation*. IEEE Transactions on Industry Electronics, Vol. 55, No. 5, 2008, pp. 1361-1368.

[17] B. Yazıcı and G. B. Kliman, *An adaptive statistical Time– Frequency method for detection of broken bars and bearing faults in motors using stator current*. IEEE Transactions on Industry Applications, Vol. 35, No 2, 1999, pp. 442-452.

[18] H. Ocak, and K. A. Loparo, *Estimation of the running speed and bearing defect frequencies of an induction motor from vibration data*. Mechanical Systems and Signal Processing, Vol. 18, No. 3, 2004, pp. 515–533.

[19] W. Zhou, T. G. Habetler and R. G. Harley, *Stator current-based bearing fault detection techniques: a general review*. IEEE Power Electronics and Drives (SDEMPED), 2007, pp. 7-10.

[20] B. Li, M. Chow, Y. Tipsuwan and J. Hung, *Neural-network-based motor rolling bearing fault diagnosis*. IEEE Transactions on Industry Electronics, Vol. 47, No. 5, 2000, pp. 1060-1069.

[21] Mohammed, O.A., Abed, N.Y. and Garni, S.C., *Modeling and characterization of induction motor internal faults using finite element and discrete wavelet transforms*. IEEE Transactions on Magnetics, Vol. 42, No. 10, 2006, pp. 3434-3436.